

SYMMETRY CONSTRAINTS AND THE ELECTRONIC STRUCTURES OF A QUANTUM DOT WITH THIRTEEN ELECTRONS

G.M. Huang, Y.M. Liu, and C.G. Bao

The State Key Laboratory of Optoelectronic Materials and Technologies,
and

Department of Physics, Zhongshan University, Guangzhou, 510275, P.R.
China

ABSTRACT: The symmetry constraints imposing on the quantum states of a dot with 13 electrons has been investigated. Based on this study, the favorable structures (FSs) of each state has been identified. Numerical calculations have been performed to inspect the role played by the FSs. It was found that, if a first-state has a remarkably competitive FS, this FS would be pursued and the state would be crystal-like and have a specific core-ring structure associated with the FS. The magic numbers are found to be closely related to the FSs.

PACS(numbers): 73.61.-r

1, INTRODUCTION

Modern experimental techniques, e.g., by using electrostatic gates and by etching, allow a certain number of electrons to be confined in semiconductor heterostructures.¹⁻⁶ Such many-electron systems have much in common with atoms, yet they are man-made structures and are usually called "quantum dot". The number of electrons contained in a dot ranges from a few to a few thousands, they are confined in a domain one hundred or more times larger than the atoms. Thus, in addition to atoms, nuclei, ... that exist in nature, quantum dots as a new kind of system will definitely contain new and rich physics, and therefore they attract certainly the interest of academic research.

On the other hand, the properties of the dots can be changed in a controlled way, e.g., by changing the gate voltage or by applying an adjustable magnetic field, etc. Therefore, these systems have a great potential in application. Due to this fact, the investigation of quantum dots is a hot topic in recent years¹⁻⁶. In the experimental aspect, progress has been made to reveal different kinds of physical property. A crucial point is to clarify the electronic structures. An important step along this line is the

first observation of the Coulomb blockade spectra via the measurement of conductance as a function of gate voltage⁷, where very clear level structure has been demonstrated. Afterwards, a substantial amount of information is drawn from conductance measurement. The measurement of the difference in chemical potential exhibits also clear shell structures⁸. The excitation of electron can be probed by far-infrared and capacitance spectroscopy.^{9,10} With further progress in experimental techniques, the dots will definitely be understood better and better, and they will serve as a rich source of information on many-body physics in the coming years.

In the theoretical aspects, detailed information on electronic structures has been obtained for the systems with a smaller N (say, $N < 10$)^{2,4,6}. When N is small, the effect of symmetry was found to be very important, e.g., the magic angular momenta of few-electron dots originate from the constraint of symmetry¹¹⁻¹³. When N is larger (say, $N \geq 10$), the effect of symmetry is scarcely studied. The systems with a larger N are themselves very attractive, because they might possess both the features of few-body and many-body systems. Thus the understanding of these systems might serve as a bridge to connect few-body and many-body physics. In a previous paper, the electronic structures of a dot with nine electrons have been studied¹³. The present paper is a continuation of the previous one, and is dedicated to the study of the dot with $N=13$ and with the spins polarized. The choice of thirteen is rather arbitrary, just because it is explicitly larger than the systems with $N < 10$ which have already been extensively studied, and because it is not very large so that accurate numerical calculations (in the qualitative sense) and detailed analysis can still be performed. From a previous study by a number of authors¹³⁻¹⁸, it is believed that a general picture of dots would consist of a core surrounding by a ring. It would be interesting to see, when N is larger, how the details of the core-ring structure would be and how these structures are affected by symmetry. Such a study would exhibit further insight of many-body physics.

In what follows, the 13-body Schrödinger equation is solved via an exact diagonalization of the Hamiltonian, the accuracy has been evaluated. The underlying dynamical and symmetry background has been studied. Favorable structures for each state have been suggested based on symmetry consideration. The eigenwavefunctions have been analyzed in detail to exhibit how the electronic structures are affected by symmetry. The appearance of magic numbers is discussed.

2, HAMILTONIAN AND THE APPROACH

Let the electrons be fully polarized (therefore the spin-part can be neglected and the spatial wave functions are totally antisymmetric) , and confined in a 2-dimensional plane by a parabolic confinement. The Hamiltonian reads

$$H = T + U \quad (1.1)$$

$$T = - \sum_{j=1}^N \frac{\hbar^2}{2m^*} \nabla_j^2 \quad (1.2)$$

$$U = \sum_{j=1}^N \frac{1}{2} m^* \omega_o^2 r_j^2 + \frac{e^2}{4\pi\epsilon_r\epsilon_0} \sum_{j<k}^N \frac{1}{r_{jk}} \quad (1.3)$$

where m^* is the effective electron mass, ϵ_r is the dielectric constant, and $\hbar\omega_o$ measures the strength of the parabolic confinement (ω_o arises mainly from a magnetic field B . This field leads also to a term linearly proportional to B . This term has been neglected because it does not at all affect the eigenwavefunctions, and therefore not affect the electronic structures).

In order to diagonalize the Hamiltonian, a set of orthonormalized single-particle harmonic oscillation (h.o.)states ϕ_{mk} are introduced. Here, ϕ_{mk} is an eigenstate of a pure h.o. Hamiltonian

$$h = -\frac{\hbar^2}{2m^*} \nabla^2 + \frac{1}{2} m^* \Omega_0^2 r^2 \quad (2)$$

where Ω_0 is an adjustable parameter in general not equal to ω_o , This eigenstate has eigenenergy $(m+k+1)\hbar\Omega_0$ and angular momentum $(m-k)\hbar$. From them the many-body basis functions (BFs)

$$\psi_\alpha(1, 2, \dots, N) = \frac{1}{\sqrt{N!}} \begin{vmatrix} \phi_{m_1 k_1}(\vec{r}_1) & \phi_{m_1 k_1}(\vec{r}_2) & \cdots & \phi_{m_1 k_1}(\vec{r}_N) \\ \phi_{m_2 k_2}(\vec{r}_1) & \phi_{m_2 k_2}(\vec{r}_2) & \cdots & \phi_{m_2 k_2}(\vec{r}_N) \\ \cdots & \cdots & \cdots & \cdots \\ \phi_{m_N k_N}(\vec{r}_1) & \phi_{m_N k_N}(\vec{r}_2) & \cdots & \phi_{m_N k_N}(\vec{r}_N) \end{vmatrix} \quad (3)$$

with a given total orbital angular momentum $L = \sum_i (m_i - k_i)$ are composed.

From the BFs, the eigenstates of the dot are expanded as

$$\Psi = \sum C_\alpha \psi_\alpha \quad (4)$$

where the coefficients C_α can be obtained via a procedure of diagonalization. The ψ_α are arranged in such a sequence that $\langle \psi_\alpha | H | \psi_\alpha \rangle \leq \langle \psi_{\alpha+1} | H | \psi_{\alpha+1} \rangle$. Evidently, in such a sequence, the ψ_α with a smaller α is more important to the low-lying states, while those with a very large α can be neglected. The H will be diagonalized step by step. In the first step,

H is diagonalized in a smaller space with N_a BFs (ψ_1 to ψ_{N_a}). Then, H is diagonalized again in a larger space with N_b BFs (from ψ_1 to ψ_{N_b} , and N_b is considerably larger than N_a). This process repeats again and again until a satisfactory convergency of the lower eigenenergies is achieved. In the first step, all the ψ_α for the diagonalization is limited to the lowest Landau levels (LLL), i.e., all the $\phi_{m_i k_i}$ contained in ψ_α have $k_i = 0$. However, step by step, BFs of higher Landau levels will mixed in. In order to speed up the convergency, the Ω_0 in eq.(2) is considered as a variational parameter to optimize the lower eigenenergies emerged from the diagonalization.

In the following calculation, we have $m^*=0.067m_e$, $\hbar\omega_0=3\text{meV}$, $\varepsilon_r=12.4$ (for a GaAs dot). To show the convergency, as an example, the lowest eigenenergies with $L=82$ are obtained as 436.895, 436.806 and 436.760meV when the number of BFs are 6000, 9000, and 12000, respectively. One can see that the convergency is not very good. However, the densities calculated below by using 6000, 9000 and 12000 BFs are indistinguishable (e.g. in Fig.1). Since we are mainly interested in the qualitative aspect, the accuracy that we have achieved is sufficient.

After the diagonalization the eigenstates are obtained. The series of states having the same L is labeled as $(L)_i$. The $i = 1$ state (the lowest of the L -series) is called a first-state.

The eigenwavefunctions of a 13-electron system are complicated. In order to extract informations from them the following physical quantities are defined and calculated. They are the one-body density

$$\rho_1(r_1) = \int |\Psi_L|^2 d\mathbf{r}_2 d\mathbf{r}_3 \cdots d\mathbf{r}_{13} \quad , \quad (5a)$$

the two-body density

$$\rho_2(\mathbf{r}_1, \mathbf{r}_2) = \int |\Psi_L|^2 d\mathbf{r}_3 d\mathbf{r}_4 \cdots d\mathbf{r}_{13} \quad , \quad (5b)$$

and the three-body density

$$\rho_3(\mathbf{r}_1, \mathbf{r}_2, \mathbf{r}_3) = \int |\Psi_L|^2 d\mathbf{r}_4 d\mathbf{r}_5 \cdots d\mathbf{r}_{13} \quad , \quad (5c)$$

It was found that in many cases the $\rho_1(r)$ has an outer peak and an inner peak with a minimum lying in between (at $r = a$). In this case we can define an outer region ($r \geq a$) and an inner region ($r < a$). Accordingly, we can define the average number of particles N_{out} and N_{in} contained in the outer and inner regions, respectively, as

$$N_{out} = N \int_a^\infty \rho_1(r_1) d\mathbf{r}_1 \quad (6a)$$

$$N_{in} = N \int_0^a \rho_1(r_1) d\mathbf{r}_1 \quad (6b)$$

For example, the $(88)_1$ state has $a = 367.8 \overset{\circ}{\text{A}}$, $N_{out} = 9.97$ and $N_{in} = 3.03$.

Once the border a is defined, we can define the angular momenta l_{out} and the moments of inertia I_{out} contributed by the outer region, respectively , as

$$l_{out} = N \int_a^\infty d\mathbf{r}_1 \int \Psi_L^* \hat{l}_1 \Psi_L d\mathbf{r}_2 \cdots d\mathbf{r}_{13} \quad (7)$$

and

$$I_{out} = M \int_a^\infty \rho_1(r_1) r_1^2 d\mathbf{r}_1 \quad (8)$$

where $M = Nm^*$ is the total mass. Similarly, the l_{in} and I_{in} contributed from the inner region can also be defined. Although these quantities are not good quantum numbers, they can help us to understand better the physics as shown later.

3, DYNAMICAL AND SYMMETRY BACKGROUND

Quantum mechanic systems are affected by both dynamical reasons and symmetry consideration . The following points are noticeable:

(i) **Core-ring structures.**

The spatial wave functions of low-lying states are mainly distributed in an area where the total potential energy U (eq.(1.3)) is lower. In particular, they would like to be distributed surrounding the (local)minima of U . In order to find out the (local)minima, let N_{in} electrons be contained inside to form a core, and N_{out} electrons be contained outside to form a ring, $N_{in}+N_{out} =N$. When the relative locations of the electrons are appropriately adjusted (e.g., they form two homocentric regular polygons with or without an electron at the center) U will be optimized and arrives at its (local) minimum U_{opt} , the associated configuration is called an $N_{in}-N_{out}$ core-ring configuration. In this configuration, let the ratio of the radii of the outer polygon and the inner polygon be denoted as G_{opt} . U_{opt} and G_{opt} are given in Table 1.

Table 1, The optimal values U_{opt} and the associated G_{opt} of the (local)minima of U , each is associated with a $N_{in}-N_{out}$ core-ring configuration.

$N_{in}-N_{out}$	1-12	2-11	3-10	4-9	5-8	6-7	7-6	8-5
U_{opt} (meV)	281.41	278.35	274.83	274.22	274.93	276.31	275.73	278.76
G_{opt}		3.73	2.83	2.41	2.16	2.02	1.77	1.70

Evidently, a too small or too large N_{out} (say, $N_{out} \leq 7$ or $N_{out} \geq 11$) is not advantageous to binding. Furthermore, the outer polygon should be neither too close to nor too far away from the core.

In what follows, when the wave function of a state is distributed

surrounding a $N_{in}-N_{out}$ core-ring configuration, then the state is said to have a $N_{in}-N_{out}$ structure. If the configuration has an electron at the center, then the structure is further denoted as $(N_{in})_c-N_{out}$, otherwise as $(N_{in})_h-N_{out}$. The subscript h implies a hollow structure.

It is shown in the table that the U_{opt} of a number of configurations are quite close to each other. At a first glance, one might expect that a strong mixing of geometric configurations would occur and would spoil the crystal-like picture. However, this is not true mainly due to the quantum constraints as we shall see later.

(ii) **Uniform rotation .**

Let us consider first a classical model system of two rotating homocentric rings. the outer ring has ($b \leq r \leq a$), while the inner ring has ($d \leq r \leq c$, and $c \leq b$). Let the angular momentum, the moment of inertia and the angular velocity of the outer (inner) ring be l_{out} , I_{out} and ω_{out} (l_{in} , I_{in} and ω_{in}), respectively. The total angular momentum $L = l_{out} + l_{in} = I_{out}\omega_{out} + I_{in}\omega_{in}$, and the total rotation energy $T = \frac{1}{2}(I_{out}\omega_{out}^2 + I_{in}\omega_{in}^2)$. Now, let us ask how the ω_{out} and ω_{in} would be chosen so that T is minimized under the condition that L is conserved? The answer is simply $\omega_{out} = \omega_{in} = L/(I_{out} + I_{in}) = L/I$. This fact implies that if the two rings are rotating with the same angular velocity, the rotation energy can be reduced. Although this point is viewed from classical mechanics, however the first-states of a quantum mechanic system would do its best to lower the energy, thus they would pursue a uniform rotation, i.e., $\omega_{out} \approx \omega_{in}$.

From the point of view of quantum mechanics, the low-lying states are mainly dominated by the BFs belonging to the LLL. In these BFs, all the single-particle state ϕ_{mk} have $k = 0$ and angular momentum $l = m - k = m$. For each ϕ_{mk} , the angular velocity can be defined as $\omega = \langle l \rangle / (m^* \langle r^2 \rangle)$, which is proportional to $\frac{l}{l+1}$ if $k = 0$. Evidently, ω is close to a constant unless l is very small. Thus, for the BFs of the LLL, all the electrons rotate with similar angular velocities, and we have the uniform rotation $\omega_{out} \approx \omega_{in}$.

(iii) **Symmetry constraints and the favorable structures.**

It has been found that *inherent nodal surfaces are imposed in wave functions by symmetry, thereby the structures of quantum states are seriously affected.*^{12,19-21} In the case of 2-dimensional polarized quantum dots, it was

found that a wave function would be zero when the electrons locate at the vertexes of a regular N -side polygon if $L \neq N(j + \frac{1+(-1)^N}{4})$, where j is an integer^{6,11,22}. This constraint can be generalized to the core-ring structures. Let the ring has an angular momentum l_{out} , while the core has l_{in} . When the outer particles locate at the vertexes of a N_{out} -side polygon, and the inner particles locate at the vertexes of a N_o -side polygon ($N_o=N_{in}$ or $N_{in} - 1$, in the latter case an electron would stay at the center), then it is straight forward to prove that the wave function would be zero if

$$l_{out} \neq N_{out}(j_2 + (1 + (-1)^{N_{out}})/4) \quad (9a)$$

or

$$l_{in} \neq N_o(j_1 + (1 + (-1)^{N_o}/4) \quad (9b)$$

where j_1 and j_2 are integers. In other words, the above configuration would be prohibited if $l_{out} (l_{in})$ does not relate to $N_{out} (N_o)$ in the above way. Thus, a $(N_{in})-N_{out}$ structure would be pursued by a first-state only if the L can be divided as a sum of l_{in} and l_{out} so that the requirements (9a) and (9b) are fulfilled. If this happens, the $(N_{in})-N_{out}$ structure is called a candidate of favorable structure (CFS) of the state. Incidentally, for an eigenstate, both the l_{out} and l_{in} are not good quantum numbers, they appear as the angular momenta of the main component of eigenwavefunctions.

Usually each state may have a number of CFS, some of them are not competitive due to having a too small or too large N_{out} , they can be neglected. In what follows, among the CFS of a state, if some of them have $N_{out} \geq 8$, then those with $N_{out} \leq 7$ are neglected; if all the CFS has $N_{out} \leq 7$, then all of them would be neglected except the one with the largest N_{out} ; all the CFS with $N_{out} = 12$ are neglected without exception. After the neglect, the remaining CFS are call the favorable structures (FSs), they are listed in Table 2. E.g., the $L = 86$ state has four CFS, namely the $(5)_c-8$, $(9)_c-4$, $(11)_c-2$, and $(12)_c-1$. Among them only the $(5)_c-8$ as a FS is listed in Table 2. When a state has more than three FS, only the most competitive three are listed.

(iv) Excitation of the core

This paper concerns only the low-lying states with $L \geq N(N - 1) / 2$ (or the filling factor $\nu \leq 1$), they contain mainly the BFs belonging to the LLL. In these BFs, the angular momenta of any pair of electrons can not be the same due to the Pauli Principle. Therefore, they can be denoted as $\psi_\alpha = \{l_1 l_2 \cdots l_N\}$ with $l_i < l_{i+1}$.

Since we have

$$\langle \phi_{l0} | r^2 | \phi_{l0} \rangle = (l+1) \frac{\hbar}{m^* \Omega_o}, \quad (10)$$

the spatial distribution of the wave function ϕ_{l0} depends on l . The smaller the l , the smaller the size. Thus, for the ψ_α belonging to the LLL, l_{in} is just equal to $l_1 + l_2 + \dots + l_{N_{in}}$. If $l_1 = 0$, there must be an electron staying at the center, because the ϕ_{00} wave function is distributed closely surrounding the center. Thus, a $(N_{in})_c$ - N_{out} structure must be contributed by the ψ_α with $l_1 = 0$, while a $(N_{in})_h$ - N_{out} structure is contributed by those with $l_1 > 0$. When all the l_i of the inner electrons satisfies $l_i + 1 = l_{i+1}$, the inner electrons are said to be compactly aligned. Meanwhile, l_{in} would arrive at its lower bound $(l_{in})_b = N_{in}(N_{in} - 1) / 2$, if $l_1 = 0$. In this case, we say that the core is inert (not excited). Otherwise, we have $l_{in} > (l_{in})_b$, and we say that the core is excited. Evidently, all the hollow states must have $l_1 > 0$, thus they have an excited core.

When $L \leq 90$, core excitation is not possible (unless the electrons jump to higher LLL), therefore the first-states would have a $(N_{in})_c$ - N_{out} structure with the core inert. However, when $L > 90$, core excitation might occur. It implies two cases: (a) The inner electrons have their l_i remaining to be compactly aligned but with $l_1 = k$, and therefore have a $(N_{in})_h$ - N_{out} hollow structure. (b) The l_i of the core are no longer aligned compactly, e.g., $l_1 = 0$ while $l_2 = 2$, etc. .

It was found that, when L is not large (say, $L \leq 101$), the first-states have either an inert core or an excited compact core with $l_1 = 1$, as shown in Table 2. However, when L is large, higher core excitation with $l_1 > 1$ will emerge as shown later.

Incidentally, due to eq.(10), the compact alignment of the angular momenta also implies a compact alignment of radial positions. Thus, in the core-ring structures, the groups of inner and outer electrons may each compactly aligned. The associated BF can be simply denoted as $\{l_1 - l_{N_{in}}, l_{N_{in}+1} - l_N\}$ (e.g., $\{1,2,3, 6,7,\dots,15\} \equiv \{1-3,6-15\}$). This is called a two-bunched BF by Ruan²³ (The one-bunched BF $\{l_1 - l_N\}$ is a special case of two-bunched BF with $l_{N_{in}} = l_{N_{in}+1} - 1$). It is straight forward to prove that, for a CFS of a $\nu \leq 1$ state, among the BFs of the CFS, one and only one of them is a two-bunched BF belonging to the LLL. Thus, a simple way to find out the CFS is to look for the two-bunched BFs of a state.

(v) **Particle separation**

It is noted that the U in eq.(1.3) can be exactly rewritten as

$$U = \frac{1}{2}M\omega_o^2 R_c^2 + \sum_{j < k} u_{eff}(r_{jk}) \quad (11.1)$$

Where R_c is the radial distance of the c.m., and $u_{eff}(r_{jk})$ is the effective pairwise interaction

$$u_{eff}(r_{jk}) = \frac{(m^*\omega_o)^2}{2M} r_{jk}^2 + \frac{e^2}{4\pi\epsilon_r\epsilon_0} \cdot \frac{1}{r_{jk}} \quad (11.2)$$

There is a minimum in u_{eff} located at $r_{jk} = r_u = \left(\frac{e^2 M}{4\pi\epsilon_r\epsilon_0(m^*\omega_o)^2}\right)^{1/3}$. Evidently, if each electron separates from all its adjacent electrons by this distance, the potential energy can be minimized. Therefore, in low-lying states, adjacent electrons would roughly keep the separation r_u . With the above parameters, $r_u = 576.3 \text{ \AA}$. The r_u is a basic measure and is useful for the understanding of electronic correlation and the size of the system. Obviously, for a $(N_{in})-N_{out}$ structure, the distance between the ring and the core depends closely on r_u .

(vi) **Core-ring separation**

It is recalled that, in order to minimize the potential energy, the ring should separate from the core by an appropriate distance. In this subsection, we shall evaluate the core-ring separation by using the approximation of uniform rotation.

For a given CFS with the given N_{out} and l_{out} , let us define a quantity

$$\bar{g} = \sqrt{\frac{l_{out}/l_{in}}{N_{out}/N_{in}}} \quad (12)$$

On the other hand, we have

$$I_{out} = m^* N_{out} \langle r^2 \rangle_{ring} \quad (13)$$

(this equation is the same as eq.(8)), and a similar equation for I_{in} . Thus we have

$$\bar{g} = \sqrt{\frac{l_{out}/l_{in}}{I_{out}/I_{in}} \cdot (\langle r^2 \rangle_{ring} / \langle r^2 \rangle_{core})} = \sqrt{\frac{\omega_{out}}{\omega_{in}} \cdot (\langle r^2 \rangle_{ring} / \langle r^2 \rangle_{core})} \quad (14)$$

It is believed that the uniform rotation is a good approximation for the first-states, because they should do their best to lower the energy (this is a point remain to be checked). Under this approximation

$$\bar{g} \approx (\langle r^2 \rangle_{ring} / \langle r^2 \rangle_{core})^{1/2} \quad (15)$$

The optimal value of the right hand side of eq.(15) has been denoted as G_{opt} given in Table 1. Thus, if a FS has its \bar{g} (evaluated from the definition eq.(12)) close to G_{opt} , then the core-ring separation is appropriate and the

FS is advantageous to binding and therefore competitive. Otherwise, it is not.

The \bar{g}/G_{opt} of the FS are also listed in Table 2, many of them are found to be very close to one. E.g., the FS of the $(86)_1$ is a $(5)_c-8$ structure with $\bar{g}=2.18$, the associated G_{opt} is 2.16 (cf. Table 1), thus they are close to each other.

The above points are important to the following discussion. *When a first-state has a FS which is superior than the other FSs (or the state has only one FS), the FS is expected to be dominant. In this case the state would have a clear geometric feature arising from the $N_{in}-N_{out}$ structure of the FS, and appear to be crystal-like.* However, when a first-state has a few nearly equally competitive FSs, its structure can not be uniquely predicted. Nevertheless, the Table 2 is a key to understand the electronic structures.

Table 2, Characters of the first-state from symmetry consideration and from our calculations.

L	Favorable structures and their related features					Quantities evaluated from the ρ_1 of the first-states			
	FS	l_1	l_{in}	\bar{g}	\bar{g}/G_{opt}	a	N_{in}	l_{in}	γ
81	(10) _c -3	0	45	1.6330					
82	(9) _c -4	0	36	1.6956					
83	(8) _c -5	0	28	1.7728	1.04				
84	(7) _c -6	0	21	1.8708	1.05	2.700	6.55	21.30	0.89
85	(6) _c -7	0	15	2.0000	0.99	2.550	5.76	16.45	0.91
86	(5) _c -8	0	10	2.1794	1.01	2.288	4.65	10.52	0.93
87	(4) _c -9	0	6	2.4495	1.02	2.100	3.85	7.21	0.95
88	(3) _c -10	0	3	2.9155	1.03	1.889	3.03	4.44	0.96
89	(2) _c -11	0	1	4.0000	1.07	1.555	2.00	1.90	0.98
90	(1) _c -12	0	0			1.120	0.97	0.42	1.094
92	(6) _c -7	0	15	2.0976	1.04	2.700	6.26	19.70	0.94
93	(8) _c -5	0	28	1.9272	1.13	2.414	4.99	12.43	0.964
94	(5) _c -8	0	10	2.2913	1.06	2.377	5.01	12.51	0.967
95	(9) _h -4	0	45	1.5811		2.205	4.06	8.30	0.967
96	(4) _c -9	0	6	2.5820	1.07	2.181	3.89	7.38	0.998
97	(7) _h -6	1	28	1.6956	0.96	1.942	3.04	4.80	0.967
98	(3) _c -10	0	3	3.0822	1.08	1.926	2.91	4.19	1.012
99	(5) _h -8	1	15	1.8708	0.86	1.519	1.74	1.86	0.904
100	(2) _c -11	0	1	4.2426	1.14	1.611	1.90	1.98	0.981
100	(4) _h -9	1	10	2.0000	0.83				
101	(3) _h -10	1	6	2.1794	0.77	1.936	2.82	6.54	0.813

4, EIGENENERGIES

After performing the diagonalization, eigenenergies and eigenstates are obtained. Let $E((L)_i)$ be the energy of the $(L)_i$ state. It is noted that , for a first-state, if the Coulomb repulsion among the electrons are removed, all the electrons would fall in the LLL with the energy $(L + N)\hbar\omega_o$. For this reason, let us define $\varepsilon(L) \equiv E((L)_1) - (L + N)\hbar\omega_o$. This quantity is a measure of the Coulomb repulsion in the first-states, which is plotted in Fig.2 in accord with L . When L increases, the size of the system will increase a little , the Coulomb repulsion will thereby decrease. Thus, $\varepsilon(L)$ decreases monotonously with L as shown in the figure. However, there are four platforms. We shall return to this point later.

5, ELECTRONIC STRUCTURES ($78 \leq L \leq 90$)

In what follows mainly the results of the first-states are given. We use $a_M \equiv \sqrt{\frac{\hbar}{m^* \omega_o}} = 194.71 \text{ \AA}$ as the unit of length. The optimal separation $r_u = 2.96 a_M$.

Let us begin from the state with the filling factor $\nu = 1$, namely the $(78)_1$ state. This state has only one BF $\{0,1,2,\dots,12\}$ (for short, $\{0-12\}$) belonging to the LLL, this BF has a weight 85.5%. In this BF, the electrons are roughly uniformly distributed inside a circle as shown in Fig.3a. It is noted that a clear geometric structure arises from the coherent mixing of BFs. Due to the lack of mixing, the $(78)_1$ can not have a clear geometric structure, therefore it is liquid-like as shown in Fig.4a.

On the other hand, for the number N together with two arbitrary integers n ($\leq N$), and j' , there is an identity

$$\frac{N(N-1)}{2} + j'N = \frac{n(n+2j'-1)}{2} + \frac{(N-n)(N+n+2j'-1)}{2} \quad (16)$$

Let the left hand side be equal to L , and the two terms at the right be equal to l_{in} and l_{out} . Then this identity is associated with a division of L . When $j' = 0$, the left hand side of (16) is equal to 78. It is easy to see that the pair $N_o = n - 1$ and l_{in} meet the requirement of eq.(9b), while the pair $N_{out} = N - n$ and l_{out} meet the requirement of eq.(9a). Thus, eq.(16) implies that all the $(N_o + 1)_c - N_{out}$ structures with $N_o = 0$ to 12 are the CFS of the $L = 78$ states. Therefore the wave function of the $(78)_1$ can get access to all the symmetric configurations^{12,13}, and thus is nodeless (except a pair of electrons overlap with each other). Accordingly, the energy of this state is lower.

For the $(79)_1$ state, there is also only one BF $\{0-11,13\}$ belonging to the LLL. Thus this state is also liquid-like as shown in Fig.4b. However, on the contrary with the $(78)_1$, all the $(N_{in}) - N_{out}$ structures are not the CFS of the $(79)_1$, except the $(12)_c - 1$ which is very poor in binding. Thus the energy of this state is much higher. Owing to the $(78)_1$ is lower while the $(79)_1$ is higher, the difference leads to a platform appearing in Fig.2 between $L = 78$ and 79.

Ranging from $(79)_1$ to $(90)_1$, all these states have only one FS, thus their structures can be well predicted. The N_{out} of their FS (cf. Table 2) increases from 1 to 12, this leads to a regular variation of their electronic structure. When N_{out} is small (say, $N_{out} \leq 5$), the outward electrons are found to be very close to the core. As a result, their ring-core-structures are ambiguous as shown in Fig.3b and 4b, where the patterns are representative

for the $(79)_1$ to $(83)_1$ states. In these states the FS itself is not competitive. This fact would lead to a stronger mixing of structures, and therefore they are liquid-like.

Even in the liquid-like states, electronic correlation can still be viewed via the three-body densities as shown in Fig.5a and 5b, they are representative. Fig.5a for the $(81)_1$ exhibits that the three outward electrons (two are labelled by white spots and one by a double-peak, which implies an oscillation around an equilibrium position) are very close to the core. This fact supports the presumption that the FS, namely the $(10)_c-3$ structure (cf. Table 2), is pursued by the state. Although the U of the $(10)_c-3$ is higher, however no other better symmetric configurations are allowed by symmetry. Consequently, the component of the $(10)_c-3$ is still relatively important. Since the outward electrons are so close, the core is strongly deformed. There are three peaks at the outer ridge of the core, it implies that three inward electrons form a regular triangle close to the border. Fig.5b for the $(82)_1$ exhibits that the four outward electrons are also very close to the core. This fact supports again that the FS is pursued. The core is also strongly deformed with four inward electrons forming a square close to the border.

The pursuit of the FS can also be viewed by observing the composition of the wave functions. For the $(81)_1$, the BF with the largest weight (35.4%) is the $\{0-9,11-13\}$, in which the electrons are divided into two compact bunchs, and therefore supports directly the $(10)_c-3$ structure. For the $(82)_1$, the BF with the largest weight (33.4%) is the $\{0-8,10-13\}$.

When $L \geq 84$, the N_{out} of the FS is ≥ 6 . Since the outward electrons would separate (roughly by r_u) from each other, a larger N_{out} definitely leads to a larger ring. Consequently, the outward electrons are no more close to the core, and the ring-core structure becomes explicit. This is shown in Fig.3c to 3f for the $(84)_1$ to $(90)_1$ states, where the outward peak becomes larger and larger. The point a separating the inner and outer regions can be well defined. Accordingly, the quantities related to eq.(6) to (8) can be calculated as listed in Table 2. In particular, a quantity related to the uniformity of rotation

$$\gamma = \frac{l_{out}}{l_{in}} / \frac{I_{out}}{I_{in}} = \omega_{out} / \omega_{in} \quad (17)$$

is defined and is also listed.

It is exhibited in Table 2 that, in the range $84 \leq L \leq 90$, a and N_{in} are decreasing. This coincides with the reduction of the core of the FS. In

particular, the N_{in} of the FS are one-to-one close to the N_{in} from calculation. This fact confirms that the FSs are pursued by the first-states. In general the N_{in} and l_{in} deviate more or less from those of the FS, this is due to the mixing of the FS together with other minor structures (the inner electrons may occasionally go out ,or the core may get slightly excited). E.g., the wave function of the $(87)_1$ has $N_{in} = 3.85$ and $l_{in} = 7.21$, while its FS has $N_{in}=4$ and $l_{in}=(l_{in})_b =6$ (incidentally, a core-excitation may cause a big increase of l_{in}). Furthermore, the γ are close to the unity, it implies that the rotation is roughly uniform. However, the slight deviation of γ implies that the system is not entirely rigid.

It is recalled that the ρ_2 of the $L \leq 83$ first-states appear as liquid-like. However, when N_{out} is neither very small nor very large (say, $6 \leq N_{out} \leq 10$), the U of the core-ring structure is lower, and thereby the associated FS becomes more dominant. This would lead to a clear crystal-like picture as shown in Fig.4c to 4g, where the outward electrons form a regular polygon. The number of vertexes (from 6 to 10) is just equal to the N_{out} of the FS. This fact once again demonstrates the pursuit of the FSs. In general, the crystal-like structure can be seen more clearly if ρ_3 is observed as shown in Fig.5c.

When N_{out} is larger than 10, due to the rapid increase of U , the associated $(N_{in})-N_{out}$ structure is no more dominant, and therefore the crystal-like picture becomes ambiguous again due to the mixing of structures. This is shown in Fig.4h and 4i.

6, ELECTRONIC STRUCTURES ($91 \leq L \leq 101$)

Inserting $j' = 1$ into eq.(16) and using the same argument as before , it is straight forward to prove that the CFS of the $L = \frac{N(N-1)}{2} + N = 91$ states include all the hollow $(N_{in})_h-N_{out}$ structures ranging from $N_{in} = 0$ to 12 . Therefore the $(91)_1$ would be nodeless if the core is hollow. On the other hand, if the core is inert, all the $(N_{in})_c-N_{out}$ are not the CFS (except the $(12)_c-1$). Thus, the $(91)_1$ is expected to be hollow . This suggestion is confirmed by Fig.3g. Similar to the $(78)_1$, the $(91)_1$ is also mainly contributed by a single BF {1-13} with the weight 82.0% . Due to the lack of coherent mixing, the $(91)_1$ is liquid-like as shown in Fig.4j.

For the first-states with $92 \leq L \leq 101$, we have

(i) The core-ring structure is explicit as representatively shown by

the ρ_1 plotted in Fig.3h to 3j. However, the core may be excited and the probability of an electron staying at the center is smaller (3i and 3j).

(ii) It is noted that a state with a large L would pursue a larger moment of inertia to reduce the rotation energy. Since the structures with $N_{out} < 7$ have a smaller moment of inertia, these structures are never found in the first-states with $L \geq 93$. Specifically, the $(92)_1$ is found to have $N_{out}=7$ as shown in Fig.4k.

(iii) Each of the $(92)_1$, $(94)_1$, $(96)_1$, and $(98)_1$ states has only one FS, this FS has an appropriate N_{out} , and has $\bar{g}/G_{opt} \approx 1$. Therefore these FSs are competitive and are expected to be dominant. This point is confirmed by the associated ρ_2 (cf. Fig.4), where a crystal-like picture with the N_{out} -side polygons is seen. Furthermore, the N_{in} of the FS of the above four states are 6, 5, 4, and 3 (cf. Table 2), while the N_{in} are 6.26, 5.01, 3.89, and 2.91, respectively. These values are one-to-one close to each other. Thus, the pursuit of the FSs is further confirmed. Besides, the FS of the above four states have $l_{in} = (l_{in})_b$, namely 15, 10, 6, and 3 (cf. Table 2), respectively. The corresponding l_{in} calculated from ρ_1 are 19.70, 12.51, 7.38, and 4.19, respectively. The latter set are always one-to-one bigger than the former set due to having a slight core-excitation.

(iv) When $L \geq 100$, the excited core (i.e., $l_{in} > (l_{in})_b$) begin to compete seriously with the inert core. For the $L = 100$ states, the competing FSs are the $(4)_h-9$ and $(2)_c-11$ as shown in Table 2. The \bar{g}/G_{opt} of the former (latter) is considerably smaller (larger) than one. It is noted that, when L is large, the outer ring would shift a little outward to increase the moment of inertia to reduce the rotation energy. Thus, a small increase of \bar{g} is of advantageous, while a decrease of \bar{g} is not. In fact, it is the $(2)_c-11$ wins in the competition and is pursued by the first-state, while the $(4)_h-9$ is pursued by the second-state. This is shown in Fig.3h and 3i, and in Fig.4o and 4p. For the $(101)_1$, the $(3)_h-10$ is the only FS, and is expected to be dominant as shown in Fig.3j and 5d.

(v) For the $(93)_1$, $(95)_1$, and $(97)_1$, the N_{out} of their FS are smaller than 7 and therefore is not competitive. Although the $(99)_1$ has $N_{out}=8$, however its \bar{g}/G_{opt} is quite small. Thus these four states do not have a competitive FS, and therefore do not have a clear-cut geometric structure to pursue. They are liquid-like. Nonetheless, their ρ_1 are more or less similar to Fig.3h, thus they still have clear core-ring structures.

(vi) All the first-states with $92 \leq L \leq 101$ rotate uniformly, they have

$\gamma \approx 1$ except the $(99)_1$ and $(101)_1$. The FSs of these two states have a considerably smaller \bar{g}/G_{opt} (cf. Table 2). Thus, due to eq.(14), if they rotate uniformly the ring would be too close to the core. To avoid being too close, ω_{out} would decrease a little. In this way, although the rotation energy may increase a little, the potential energy may thereby considerably decrease. This suggestion is confirmed by the fact that their γ is really smaller. Incidentally, since the angular momentum l_{out} is strongly constrained by symmetry via eq.(9a), and therefore can not be adjusted freely, the decrease of ω_{out} would cause an increase of I_{out} via the relation $l_{out} = I_{out}\omega_{out}$.

7, ELECTRONIC STRUCTURES ($L \approx 200$)

The main finding of the above study is the pursuit of the FSs. Does this experience work when L is much larger? To clarify this point we shall no more go to the states one-by-one, instead we choose arbitrary a range $196 \leq L \leq 201$ for the studying. Let us first evaluate the accuracy of the calculation in this range. E.g., the energies of the $(199)_1$ state calculated with 6000, 9000, and 12000 BFs, respectively, together with the α , N_{in} , l_{in} and γ are listed in Table 3. One can see that, although the convergency is not very good, it is qualitatively acceptable.

Table 3 The energies and the quantities extracted from the ρ_1 of the $(199)_1$ in accord with the increase of the number of BFs.

Number of BFs	α	N_{in}	l_{in}	γ	$E((199)_1)$
6000	3.121	3.96	10.56	1.268	739.97
9000	3.123	3.97	10.75	1.238	739.86
12000	3.125	3.98	10.86	1.227	739.81

The FSs are shown in Table 4. The FSs with the core inert ($l_1 = 0$) are found to have a too large \bar{g}/G_{opt} , and therefore are not listed. Whereas an excited core is pursued. On the other hand, a highly excited core ($l_1 \geq 6$) would lead to a too small \bar{g}/G_{opt} as shown in the table. Thus, too weak and too strong core-excitation are both not appropriate.

Table 4 A continuation of Table 2 for the first- states with ($196 \leq L \leq 201$).

L	Favorable structures and their related features					Quantities evaluated from the ρ_1 of the first-states			
	FS	l_1	l_{in}	\bar{g}	\bar{g}/G_{opt}	a	N_{in}	l_{in}	γ
196	$(5)_h-8$	6	40	1.5612	0.72				
196	$(3)_h-10$	6	21	1.5811	0.59	3.16	3.75	13.88	1.11
196	$(2)_h-11$	4	9	1.9437	0.52				
197	$(5)_h-8$	3	25	2.0736	0.96	3.48	4.80	24.61	1.05
197	$(4)_h-9$	5	26	1.7097	0.71				
197	$(3)_h-10$	3	12	2.1506	0.76				
198	$(4)_h-9$	3	18	2.1082	0.85	3.25	3.90	18.65	1.10
198	$(2)_h-11$	5	11	1.7581	0.47				
199	$(4)_h-9$	1	10	2.8983	1.20	3.13	3.98	10.86	1.23
199	$(5)_h-8$	5	35	1.7113	0.80				
200	$(5)_h-8$	2	20	2.3717	1.01	3.47	4.93	20.88	1.10
200	$(3)_h-10$	4	15	1.9235	0.70				
200	$(2)_h-11$	6	13	1.6172	0.43				
201	$(3)_h-10$	1	6	3.1225	1.10	3.00	3.06	7.27	1.24
201	$(2)_h-11$	1	3	3.4641	0.93				
201	$(4)_h-9$	6	30	1.5916	0.66				

For the $(196)_1$ none of the FSs are superior (their \bar{g}/G_{opt} are too small), therefore this state would have a strong mixing of structures and would be liquid-like. Among the three FSs of the $(197)_1$, the $(5)_h-8$ has its \bar{g} closer to G_{opt} , thus this FS is predicted to be dominant. Similarly, based on Table 4, the $(4)_h-9$ is predicted to be dominant in $(198)_1$ and $(199)_1$, the $(5)_h-8$ is predicted to be dominant in $(200)_1$, and the $(3)_h-10$ is predicted to be dominant in $(201)_1$. It turns out that, for the case with a dominant FS, the predictions are nicely confirmed by the calculation. E.g., the N_{in} of the above FSs of the $(197)_1$ to $(201)_1$ are 5, 4, 4, 5, and 3, while the corresponding N_{in} extracted from ρ_1 are 4.80, 3.90, 3.98, 4.93, and 3.06. The l_{in} of the above FSs are 25, 18, 10, 20, and 6, while the corresponding l_{in} extracted from ρ_1 are 24.61, 18.65, 10.86, 20.88, and 7.27. These values are amazingly one-to-one close to each other, and thus the analysis based on the FSs is convincing. Furthermore, the associated ρ_2 and ρ_3 confirm also the predictions. Representative examples are given in Fig. 4q, 4r, 5e, and 5f.

It is noted that the $(199)_1$ and $(201)_1$ have a considerably larger γ .

On the other hand, their most competitive FSs have a larger \bar{g}/G_{opt} . Thus, if these states rotate uniformly, the ring would be too far away from the core (cf. eq.(15)). To avoid being too far away, the ring rotates a little faster to reduce the moment of inertia without altering l_{out} . This is the reason why they have a considerably larger γ .

In general, when L is large, the size of the system would increase, the core-ring structures become more clear-cut. Besides, the core would have a higher excitation. As a result, all these states are hollow as shown in Fig. 3k, 3l, 5e and 5f.

8, MAGIC NUMBERS

The above discussions demonstrate that, based on the FSs, the structures of the first-states can be more or less predicted. In this section we shall see that the energies are also strongly related to the FSs. Let us go back to Fig.2 where platforms and shoulders are shown. A platform starting at L_a and ending at $L_b = L_a + 1$ implies $E((L_b)_1) = E((L_a)_1) + \hbar\omega_o$, i.e., the $(L_b)_1$ is an c.m. excited state of the $(L_a)_1$. This fact implies that the internal energy (the energy without the c.m. motion) of the $(L_b)_i$ states are relatively higher. This is also the case if a shoulder appears. In this case, L_a is a candidate of a magic number (CMN). Evidently, if the $(L_a)_1$ has a competitive FS and the $(L_b)_1$ does not have, a CMN arises. For example, the $(78)_1$ is inherently nodeless and is able to get access to all symmetric configurations, while the $(79)_1$ has only one CFS $(12)_{c-1}$ which is unfavorable to binding. Thus the 78 appears as a CMN. Similarly, the $(91)_1$ is inherently nodeless (if the core is excited), while the $(92)_1$ has only the $(6)_{c-7}$ (which is not competitive due to $N_{out} = 7$), thus 91 is a CMN. The $(111)_1$ has a competitive FS $(3)_{h-10}$. Although the $(112)_1$ has two FSs, namely the $(6)_{h-7}$ and $(5)_{h-8}$, however the former has a small N_{out} while the latter has a too small $\bar{g}/G_{opt} = 0.78$. They are both not competitive, thus 111 is a CMN. Finally, The $(118)_1$ has a number of competitive FSs, namely the $(3)_{c-10}$, $(5)_{c-8}$, and $(4)_{h-9}$, while the $(119)_1$ has only one FS $(6)_{h-7}$, which is not competitive due to having $N_{out} = 7$. Thus 118 is a CMN. These examples exhibit that the CMN can be more or less predicted.

9, SUMMARY

The electronic structures of the first-states have been studied. By an analysis of symmetry constraint and by performing numerical calculation,

we have obtained a clear picture of the core-ring structures. When L is small ($78 \leq L \leq 83$), the core and ring are connected. When L is larger than 83, the core-ring structure becomes more and more explicit. When $L \leq 100$, the core remains inert (the $(91)_1$ is an exception). When L is larger, core excitation begins to compete. When L is much larger (say, $L \approx 200$), core excitation becomes dominant and the states are hollow.

The number of particles and the amount of angular momentum contained in the core (ring) are not only determined by dynamics, but depend seriously on symmetry constraint. Due to the constraint, for a given state, it is advantageous to pursue a specific kind of structure, but disadvantageous to pursue another kind. This leads to Table 2 and 4, where the favorable structures (FSs) of each state are listed.

The identification of the FSs is the main result of this paper. Based on the FSs, the structures of the first-states can be predicted to a great extent, the formation of crystal-like structure and the appearance of magic numbers can be explained. In particular, *if a first-state has a remarkably competitive FS (both the N_{out} and \bar{g}/G_{opt} are appropriate), the FS would be pursued, and the state would be crystal-like and possess the associated $(N_{in})-N_{out}$ structure. If the $L = L_a$ states contain one or more than one competitive FSs while the $L = L_a + 1$ states do not contain, then L_a is a CMN.*

The FSs can provide us an objective base for the further classification of states. The states having the same FSs can be grouped into a kind, e.g., all the $L = 87, 96, 105, \dots$ contain a single FS $(4)_c-9$, thus they belong to the same kind and their first-states would have the same $(4)_c-9$ structure.

Although only a $N=13$ system is concerned in this paper, the idea, the way of analysis, the qualitative results are quite common to the 2-dimensional systems with an attractive center. In fact, both this paper and the previous ref.[8] provide qualitatively similar message. Thus, it is not doubted that the physical picture provided by these two papers can be generalized to the systems with an even larger N . Where, the identification of the FSs is again a key to understand the electronic structures .

Acknowledgment: This paper is supported by the NSFC of China under the grant No.90103028, No.10174098, and by a fund from the Ministry of Education of China.

REFERENCES

- 1, L. Jacak , P. Hawrylak, A. Wójs, *Quantum Dots* (Springer, Berlin, 1998)
- 2, T. Chakraborty, *Quantum Dots* (Elsevier, Amsterdam, 1999)
- 3, M.S. Kushwaha, *Surface Science Reports*, **41**, 1 (2001)
- 4, S.M Reimann and M. Manninen, *Rev. Mod. Phys.* **74**, 1283 (2002)
- 5, G.W. Bryant , *Phys. Rev. Lett.* **59**, 1140, (1987)
- 6, P.A. Maksym, H. Imamura, G.P. Mallon, and H. Aoki, *J. Phys.: Condens. Matter* **12**, R299 (2000)
- 7, U. Meirav, M.A. Kastner, and S.J. Wind, *Phys. Rev. Lett.* **65**, 771 (1990)
- 8, S. Tarucha, D.G. Austing, T. Honda, R.J. van der Haage, and L. Kouwenhoven, *Phys. Rev. Lett.* **77**, 3613 (1996)
- 9, H. Drexler, D. Leonard, W. Hansen, J.P. Kotthaus, and P.M. Petroff, *Phys. Rev. Lett.* **73**, 2252 (1994)
- 10, M. Fricke, A. Lorke, J.P. Kotthaus, G. Medeiros-Ribeiro, and P.M. Petroff, *Europhys. Lett.* **36**, 197 (1996).
- 11, W.Y. Ruan, Y.Y. Liu, C.G. Bao and Z.Q. Zhang, 1995 *Phys. Rev.* **B51** 7942 (2000).
- 12, C.G. Bao, *Phys. Rev. Lett.* **79**, 3475 (1997).
- 13, C.G. Bao, *J. Phys. :Condens. Matter* **14**, 8549 (2002)
- 14, C. de C. Chamon, and X.G. Wen, *Phys. Rev.* **B49**, 8227, (1994)
- 15, H.M. Muller and S.E. Koonin, *Phys. Rev.* **B54**, 14532, (1996)
- 16, E. Goldmann and S.R. Renn, *Phys. Rev.* **B60**, 16611, (1999)
- 17, S.M. Reimann, M. Koskinen, M. Manninen and B.R. Mottelson, *Phys. Rev. Lett.* **83**, 3270, (1999)
- 18, C. Yannouleas and U. Landman, *Phys. Rev. B* **66**, 115315 (2002)
- 19, C.G. Bao, *Few-Body Systems*, **13**, 41 (1992).
- 20, C.G. Bao and Y.X. Liu, *Phys. Rev. Lett.*, **82**, 61 (1999)
- 21, C.G. Bao, W.F. Xie, and W.Y. Ruan, *Few-Body Systems*, **22**, 135 (1997)
- 22, T. Seki, Y. Kuramoto, and T. Nishino, *J. Phys. Soc. Japan*, **65**, 3945 (1996)
- 23, Ruan W Y, Chan K S, Ho H P and Pun E Y B, 2000 *J. Phys.: Condens. Matter* **12**, 3911

Caption

Fig.1 $\rho_1(r)$ of the first-state $(82)_1$ with 6000 (a), 9000 (b), and 12000 (c) basis functions. The unit of length in this paper is $\sqrt{\hbar/m^*\omega_0} = 194.71 \text{ \AA}$.

Fig.2 $\varepsilon(L)$ as a function of L . $\hbar\omega_0=3\text{meV}$ is assumed.

Fig.3 $\rho_1(r)$ of the first-states (Fig.3i is for a second-state).

Fig.4 The contour plot of the two-body densities $\rho_2(\mathbf{r}, \mathbf{r}_2)$ as a function of \mathbf{r} . The given \mathbf{r}_2 is marked by a white spot. The lighter region has a larger ρ_2 .

Fig.5 The contour plot of the three-body densities $\rho_3(\mathbf{r}, \mathbf{r}_2, \mathbf{r}_3)$ as a function of \mathbf{r} . The given \mathbf{r}_2 and \mathbf{r}_3 are marked by two white spots. Refer to Fig.4.

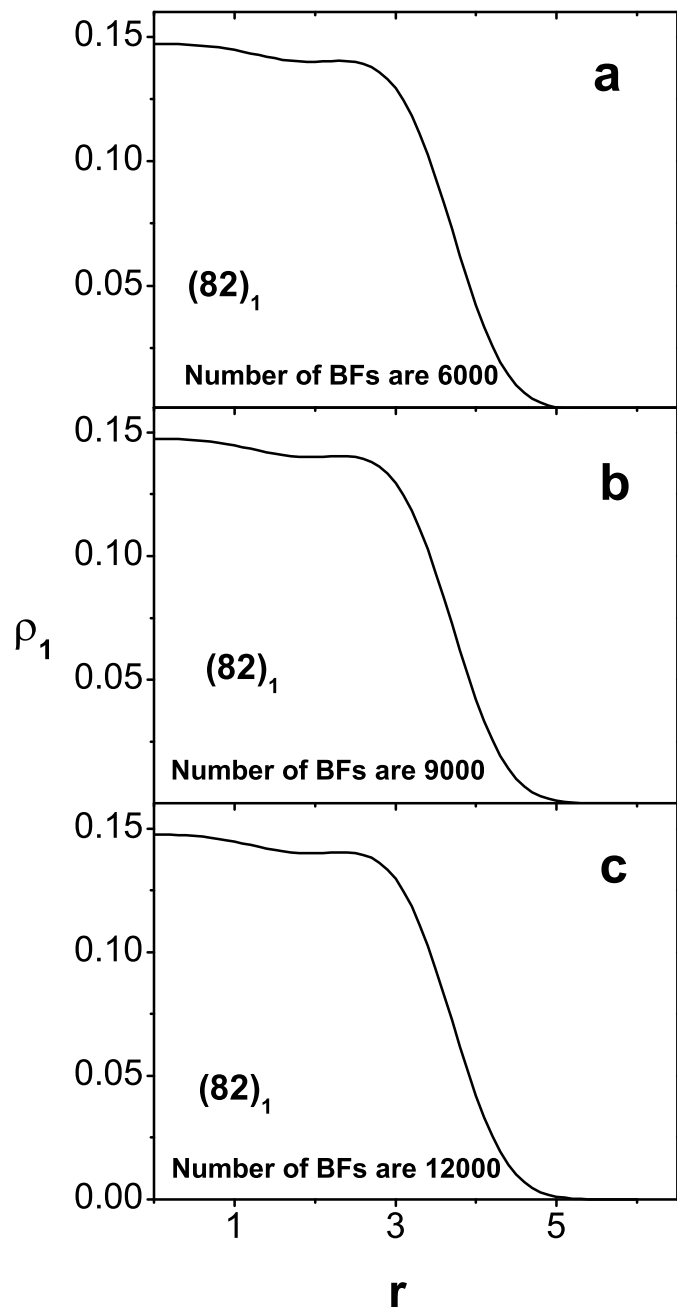


Fig.1

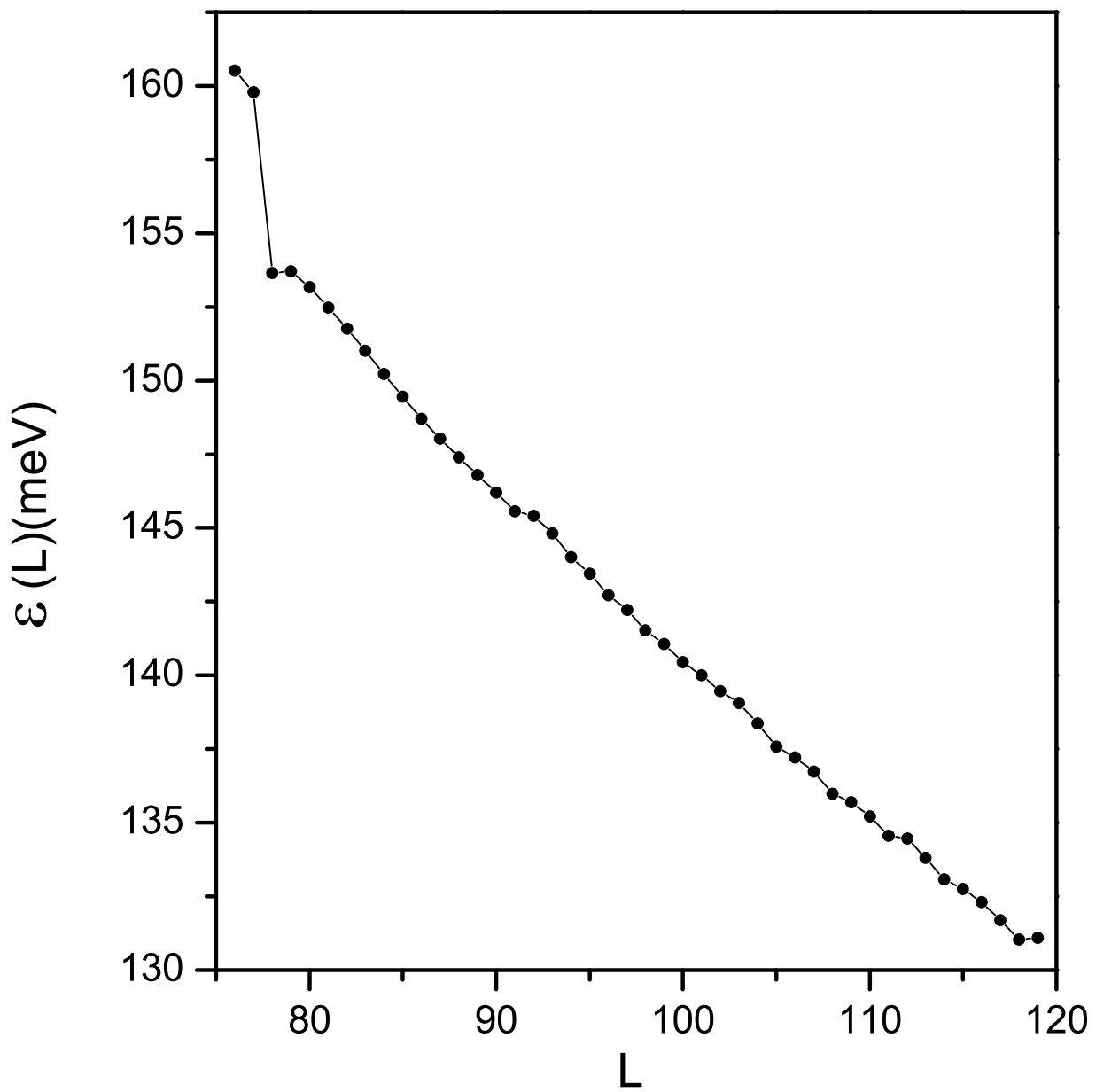


Fig.2

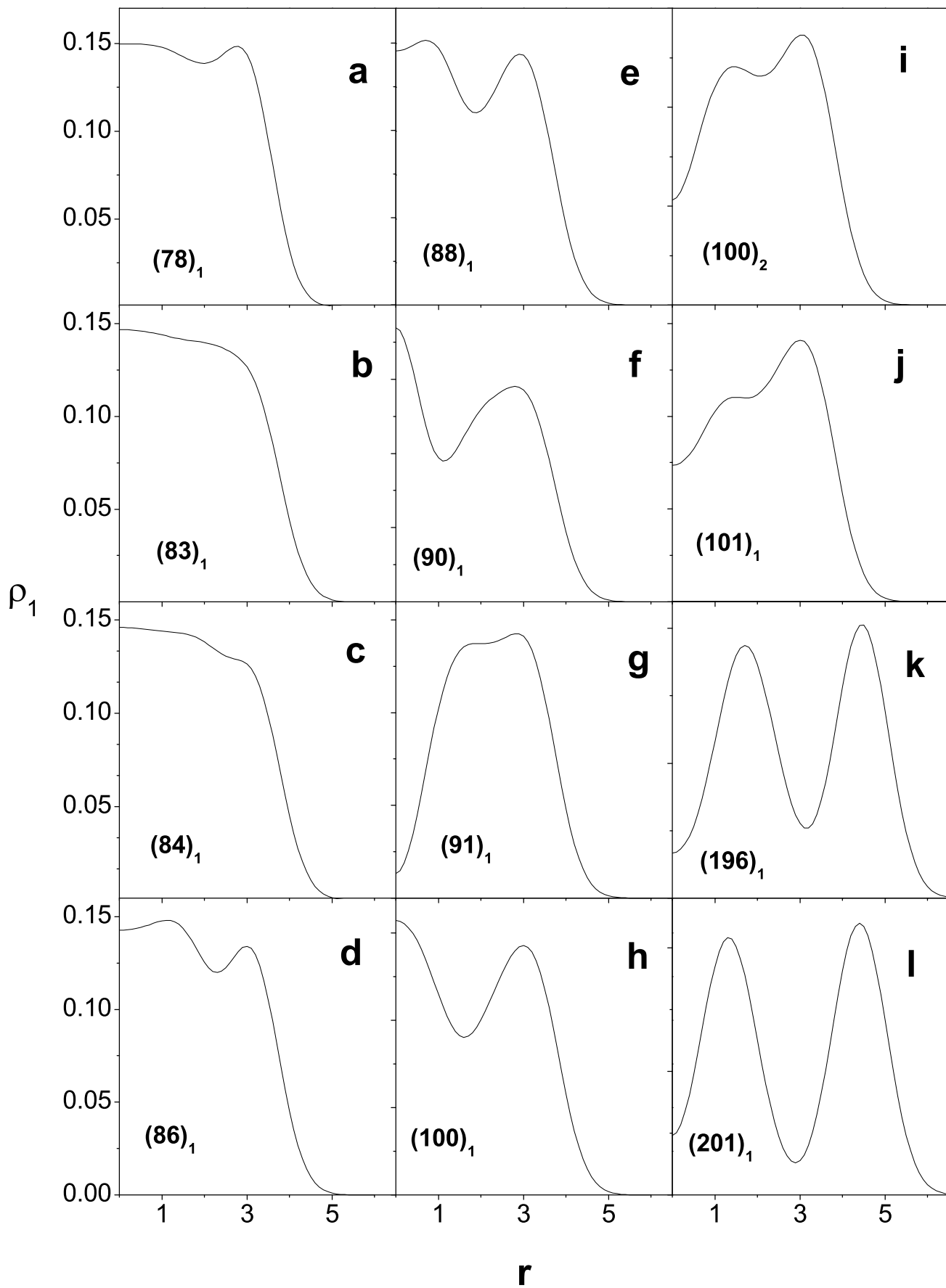


Fig.3

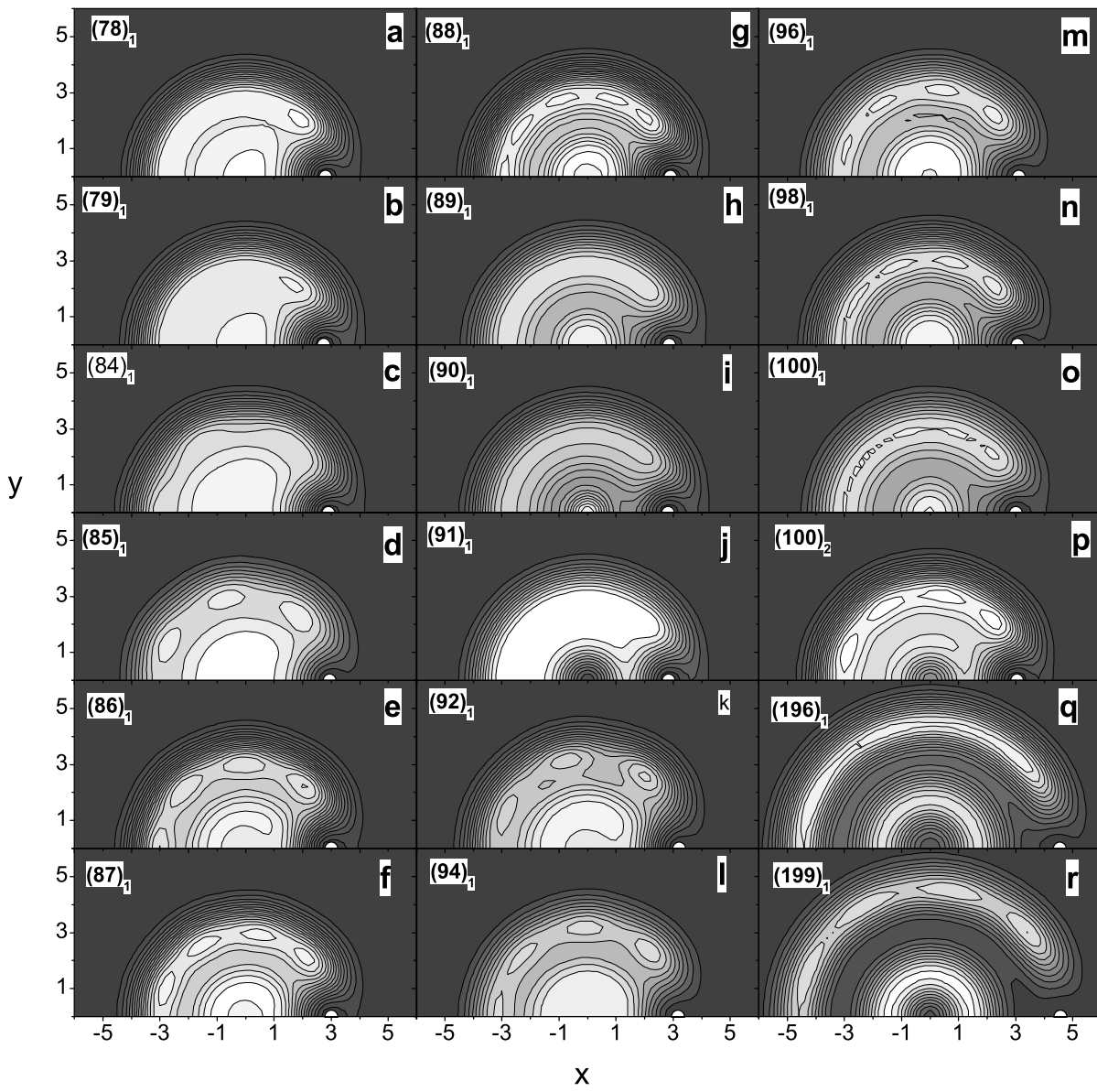


Fig.4

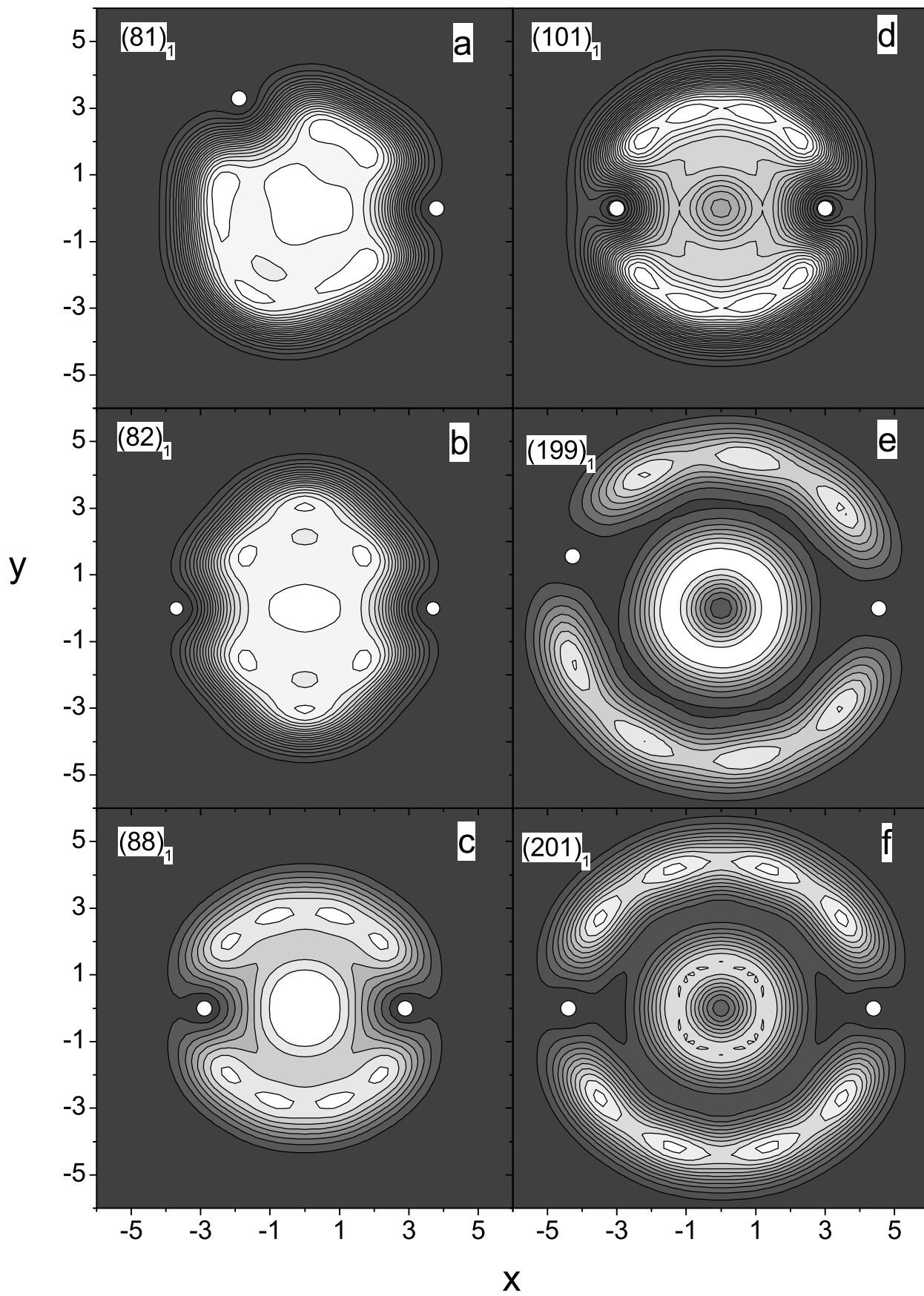


Fig.5